


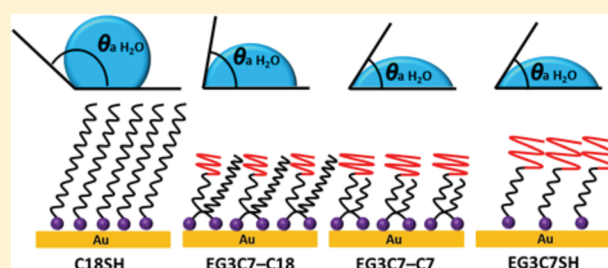
# Structure, Wettability, and Thermal Stability of Organic Thin-Films on Gold Generated from the Molecular Self-Assembly of Unsymmetrical Oligo(ethylene glycol) Spiroalkanedithiols

Pawilai Chinwangso, Han Ju Lee, Andrew C. Jamison, Maria D. Marquez, Chul Soon Park, and T. Randall Lee\*

Department of Chemistry and the Texas Center for Superconductivity, University of Houston, 4800 Calhoun Road, Houston, Texas 77204-5003, United States

## Supporting Information

**ABSTRACT:** Organic thin-films on gold were prepared from a set of new, custom-designed bidentate alkanethiols possessing a mixture of normal alkane and methoxy-terminated tri(ethylene glycol) chains. The new unsymmetrical spiroalkanedithiol adsorbates were of the form  $[\text{CH}_3\text{O}(\text{CH}_2\text{CH}_2\text{O})_3(\text{CH}_2)_5]-[\text{CH}_3(\text{CH}_2)_{n+1}\text{C}[\text{CH}_2\text{SH}]_2]$  where  $n = 3$  and 14; designated EG3C7–C7 and EG3C7–C18, respectively. Their corresponding self-assembled monolayers (SAMs) on gold were characterized and compared with monothiol SAMs derived from an analogous normal alkanethiol (C18SH) and an alkanethiol terminated with an oligo(ethylene glycol) (OEG) moiety (i.e., EG3C7SH). Ellipsometric data revealed reduced film thicknesses for the double-chained dithiolate SAMs, which perhaps arose from the phase-incompatible merger of a hydrocarbon chain with an OEG moiety, contributing to disorder in the films and/or an increase in chain tilt. The comparable wettabilities of the SAMs derived from EG3C7SH and EG3C7–C7, using water as the contacting liquid, are consistent with exposure of the OEG moieties at both interfaces, whereas the lower wettability of the SAM derived from EG3C7–C18 is consistent with exposure of hydrocarbon chains at the interface. The data collected by X-ray photoelectron spectroscopy confirmed the formation of the new OEG-terminated dithiolate SAMs, and also revealed them as less densely packed monolayers due in part to the large molecular cross section of the OEG moieties and to their double-chained structure with dual surface bonds. Mixed SAMs formed from pairs of monothiols having chain compositions analogous to those of the chains of the new dithiols showed that an EG3C7SH/heptanethiol-mixed SAM and the EG3C7–C7 SAM produced almost identical characterization data, revealing the favorable film formation dynamics for adsorbate structures where the alkyl chains can assemble beneath the phase-incompatible OEG termini. For the mixed SAM formed from EG3C7SH/C18SH, the data indicate that the EG3C7SH component failed to incorporate in the film, demonstrating that the blending of phase-incompatible chains is sometimes best accomplished when both chains exist on a single adsorbate structure. Furthermore, the results of solution-phase thermal desorption tests revealed that the OEG-terminated films generated from the bidentate EG3C7–C7 and EG3C7–C18 adsorbates exhibit enhanced thermal stability when compared to the film generated from monodentate EG3C7SH. In a brief study of protein adsorption, the multicomponent SAMs showed a greater ability to resist the adsorption of fibrinogen on their surfaces when compared to the SAM derived from C18SH, but not better than the monolayer derived from EG3C7SH.



## ■ INTRODUCTION

Poly(ethylene glycol) (PEG), which is also frequently referred to as poly(ethylene oxide) (PEO), stands as an important polymer for use in many clinical and biological applications.<sup>1</sup> PEGylated surfaces have been recognized for their outstanding protein-resistant properties and used as surface coatings to impart resistance to the adsorption of proteins and other macromolecules.<sup>1–4</sup> These features are important in technologies that involve interfacial contact between biological environments and elements such as biosensors,<sup>5,6</sup> biomolecular devices,<sup>7,8</sup> and model membranes.<sup>9,10</sup> Importantly, protein resistance does not require the use of high molecular weight PEG polymers; namely, surfaces presenting oligo(ethylene

glycol) (OEG) moieties (2–6 monomer units) have also proven effective.<sup>11–14</sup> Additionally, the surfaces of polymers are typically rough and nonuniform, making it difficult to obtain accurate and reproducible characterization data.<sup>15</sup> Therefore, self-assembled monolayers (SAMs) of OEG-terminated alkanethiols on gold have been widely used as model surfaces because well-defined organic films are formed that can be accurately and reproducibly characterized.<sup>16–23</sup> Also, these surfaces can be tailored by modifying the termini of the chains

**Received:** October 19, 2016

**Revised:** January 19, 2017

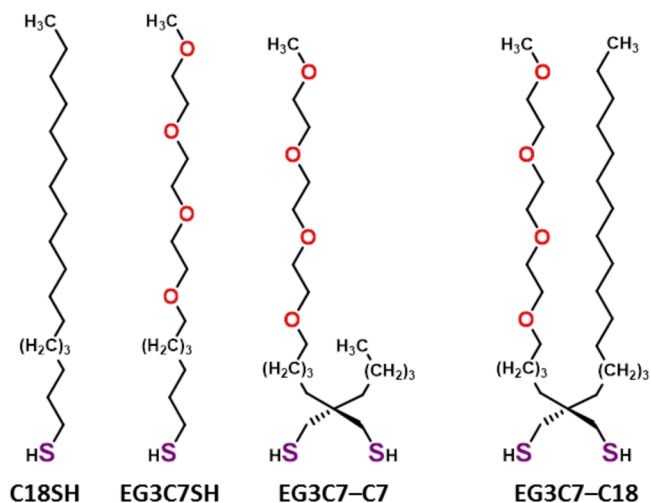
**Published:** January 20, 2017

through organic synthesis, and gold is a practical substrate for biological applications due to its high biocompatibility.<sup>16</sup>

Tri(ethylene glycol)-terminated alkanethiols on gold, in particular, have been employed in protein-resistance studies.<sup>13,17,18</sup> A report by Prime and Whitesides in 1993 revealed that the OEG chains with methoxy- and hydroxyl-termination showed similar protein resistance.<sup>13</sup> Therefore, a hydrophilic hydroxyl-terminated interface is unnecessary to prevent protein deposition on the surface. However, a single-point attachment between the alkanethiol adsorbates and the gold substrates introduces some limitations in the use of the resulting monolayer films when film stability is a major concern. For example, SAMs derived from normal alkanethiols readily decompose at elevated temperatures ( $\sim 70$  °C).<sup>19</sup> To enhance film stability, the idea of creating multiple-point attachments between each individual surfactant and the metallic substrate has been examined.<sup>24–31</sup> Such structures exhibit an entropy-driven “chelate effect” that leads to an enhanced stability for the monolayer film, similar to inorganic metal–ligand complexes.<sup>29</sup> Additionally, chelating or “bidentate” dithiols offer greater flexibility in the development of film composition than monothiols because the enhanced adsorbate stability allows for the incorporation of two different terminal components into the same adsorbate,<sup>30,31</sup> allowing the generation of homogeneously mixed multicomponent surfaces.<sup>30</sup>

The issue of homogeneous mixing is a phenomenon often overlooked in mixed monolayer systems, where chains comprised of different species spontaneously undergo phase separation to yield surfaces with single-component domains (e.g., patches, stripes, or other patterns).<sup>32–35</sup> Our group is interested in studying the behavior and properties of surfaces where such phase separation is restricted or even eliminated, affording interfaces that are comprised of chemically disparate species that are held in close proximity while preferring to be apart. We call these systems “conflicted interfaces”, and given that nature is replete with examples of heterogeneous organic interfaces (e.g., the surfaces of proteins and cells), we wish to undertake an investigation of complementary but well-defined unnatural systems starting with fundamental components of common organic thin-films, such as hydrocarbon and ethylene glycol moieties. Furthermore, ethylene glycol units are commonly found in organic thin films due to their adhesion resistance toward biological matter (e.g., proteins and cells),<sup>1–4</sup> which renders them useful in applications such as cell patterning, bioconjugation, and biosensing.<sup>5–7,21</sup>

To this end, we examine in the present study two new bidentate adsorbates possessing mixed-chain character that are based upon a combination of normal alkane and methoxy-terminated tri(ethylene glycol) chains:  $[\text{CH}_3\text{O}(\text{CH}_2\text{CH}_2\text{O})_3(\text{CH}_2)_5][\text{CH}_3(\text{CH}_2)_{n+1}]\text{C}[\text{CH}_2\text{SH}]_2$  (where  $n = 3, 14$ ; identified as EG3C7–C7 and EG3C7–C18, respectively), as shown in Figure 1. The terminal methoxy group for the OEG chains was chosen due to the ease of its incorporation during synthesis and the fact that it eliminates any complications associated with hydrogen bonds between chains that might occur with a hydroxyl group at the chain termini. These SAMs were prepared and characterized alongside SAMs formed from an analogous OEG-terminated monoalkanethiol and a normal alkanethiol, each with an equivalent number of carbon atoms as compared to the respective longest chain of the two dithiols. The monothiol adsorbates were *n*-octadecanethiol (C18SH) and methoxy-terminated tri(ethylene glycol) heptanethiol (EG3C7SH), each possessing 18 atoms in



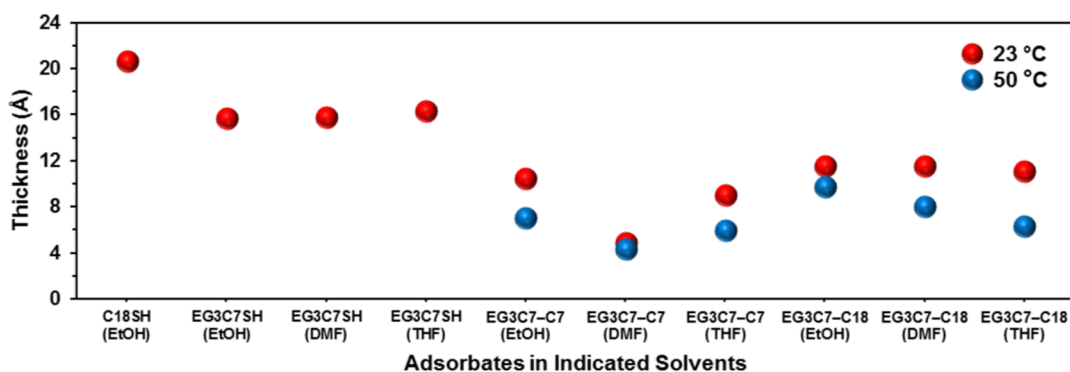
**Figure 1.** Molecular structures of the unsymmetrical oligo(ethylene glycol) spiroalkanedithiols, EG3C7–C7 and EG3C7–C18, and the corresponding monothiols, EG3C7SH and C18SH.

the backbones of their chains, if one includes both carbon and oxygen in that count (see Figure 1). For this report, the films were characterized using the instrumental methods of ellipsometry, contact angle goniometry, polarization modulation infrared reflection–absorption spectroscopy (PM-IRRAS), and X-ray photoelectron spectroscopy (XPS), along with a protein-adsorption study that provides perspective regarding the antiadhesive properties of these films toward such biomolecules.

## EXPERIMENTAL SECTION

**Nomenclature.** The abbreviations, associated names, and molecular formulas for the OEG-incorporating thiol adsorbates are EG3C7SH for 2,5,8,11-tetraoxaoctadecane-18-thiol ( $\text{CH}_3\text{O}(\text{CH}_2\text{CH}_2\text{O})_3(\text{CH}_2)_7\text{SH}$ ); EG3C7–C7 for 2-(2,5,8,11-tetraoxahexadecan-16-yl)-2-pentylpropane-1,3-dithiol ( $[\text{CH}_3\text{O}(\text{CH}_2\text{CH}_2\text{O})_3(\text{CH}_2)_5][\text{CH}_3(\text{CH}_2)_4]\text{C}[\text{CH}_2\text{SH}]_2$ ); and EG3C7–C18 for 2-(2,5,8,11-tetraoxahexadecan-16-yl)-2-hexadecylpropane-1,3-dithiol ( $[\text{CH}_3\text{O}(\text{CH}_2\text{CH}_2\text{O})_3(\text{CH}_2)_5][\text{CH}_3(\text{CH}_2)_{15}]\text{C}[\text{CH}_2\text{SH}]_2$ ). For all of the adsorbate abbreviations, the letters indicate the chemical composition of the adsorbate: EG denotes the ethylene glycol unit ( $\text{CH}_2\text{CH}_2\text{O}$ ), C denotes the methyl and methylene moieties ( $\text{CH}_3$  and  $\text{CH}_2$ ) within the hydrocarbon chain, SH denotes a monothiol structure, and “–” separates the chain abbreviations that compose the double-chained dithiol structure. The number following either C or EG indicates the number of each unit along the chain backbone (i.e., the number of each structural type between the sulfur headgroup and the terminus of the chain). In the case of a double-chained dithiol structure, a quaternary branch point carbon is counted as a methylene unit.

Complete details regarding the materials, procedures, and instrumentation used to conduct the research reported herein are provided in the Supporting Information, including the  $^1\text{H}$  and  $^{13}\text{C}$  NMR spectra for 2-(2,5,8,11-tetraoxahexadecan-16-yl)-2-pentylpropane-1,3-dithiol (EG3C7–C7) and 2-(2,5,8,11-tetraoxahexadecan-16-yl)-2-hexadecylpropane-1,3-dithiol (EG3C7–C18) (please see Figures S1–S4).



**Figure 2.** Thicknesses of the films generated from each adsorbate solution at room temperature (23 °C) and an elevated temperature (50 °C). The SAMs formed from C18SH and EG3C7SH were incubated only at room temperature (23 °C). Values were reproducible to  $\pm 2$  Å.

## RESULTS AND DISCUSSION

**I. Characterization of OEG-Terminated SAMs on Evaporated Gold Surfaces.** The solvents we chose to use as the equilibrating solvents to generate the new SAMs include tetrahydrofuran (THF), dimethylformamide (DMF), and ethanol. These choices are based on previous literature reports describing the formation of OEG- and PEG-terminated SAMs.<sup>17,36,37</sup> A longer adsorption time (48 h) than the usual time used for developing normal alkanethiols (24 h) is typically needed to generate SAMs having maximum coverage and conformational order from the dithiol-based adsorbates.<sup>30</sup> Stability studies of bidentate alkanedithiol SAMs indicate that the SAMs generated at 50 °C can resist desorption better than those generated under ambient conditions, leading to more thermally robust films.<sup>27</sup> Therefore, we also explored the formation of the OEG-terminated dithiolate films at room temperature (23 °C) and at an elevated temperature (50 °C) to evaluate whether a higher temperature would lead to enhanced film formation.

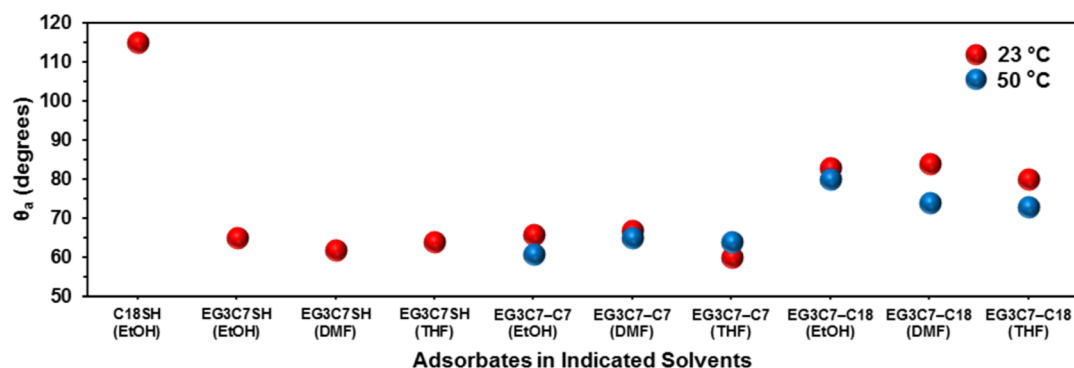
**Thicknesses of the Films.** Ellipsometry is used as a preliminary test to confirm SAM formation from the studied adsorbates. The divergence in thin-film characteristics for the two types of adsorbate chains is readily observed in the ellipsometric data generated from the monothiolate SAMs. Notably, well-formed *n*-alkanethiolate monolayers exhibit a linear alignment for the alkyl chains (i.e., all *trans*-extended),<sup>38</sup> while a similarly fully formed OEG-terminated thin film often exhibits chain termini that are subject to coiling,<sup>17,36</sup> which can lead to a reduction in the film thickness relative to an *n*-alkanethiolate SAM (*vide infra*). Table S1 in the [Supporting Information](#) provides detailed ellipsometric thickness data for the SAMs on gold derived from the OEG-terminated alkanedithiols as well as the thicknesses of the SAMs derived from the monothiols. To assist in the comparison of the data, we plotted the data in [Figure 2](#). The average thickness measurement from the C18SH SAMs is in line with previously reported values, reflecting the *trans*-extended conformation of the carbon backbone with a tilt angle of  $\sim 30^\circ$  from the surface normal.<sup>38</sup> In the case of the EG3C7SH SAMs, the thicknesses of the monolayers derived from all three solvents were comparable, indicating similar structures for these films despite the different equilibrating solvents. The structure of the OEG-terminated alkanethiolate SAMs on gold has been probed by Fourier transform infrared reflection–absorption spectroscopy (FT-IRRAS) in the work reported by Harder et al.<sup>17</sup> These authors concluded that the OEG moieties adopt helical conformations with the OEG segment oriented nearly

perpendicular to the surface, positioned on top of the underlying *trans*-extended alkyl chain, which is tilted  $\sim 30^\circ$  from the surface normal. This structural arrangement produces incremental thicknesses of 1.10 and 2.78 Å per methylene unit and EG unit ( $-\text{OCH}_2\text{CH}_2-$ ), respectively.<sup>17</sup> According to the proposed conformation, we were able to predict the thickness of the EG3C7SH film to be  $\sim 17$  Å,<sup>36,39</sup> which compares well with the data provided in [Table S1](#), and within the experimental uncertainty of the ellipsometric measurements ( $\pm 2$  Å).

Regarding the double-chained dithiolate SAMs formed at room temperature, the EG3C7–C18 and EG3C7–C7 SAMs had lower film thicknesses as compared to the corresponding EG3C7SH SAM. These results probably correlate with the differences in film structure and/or chain orientation for each adsorbate. Due to the unfavorable interactions between the hydrocarbon (C18–, hydrophobic) and OEG-terminated alkyl (EG3C7–, hydrophilic) components in the EG3C7–C18 SAM, it is possible that there is considerable chain disorder in this film, which likely reduces adsorbate packing and might give rise to a general increase in the chain tilt from the surface normal for the individual chains as compared to the C18SH and EG3C7SH analogues, thus contributing to the formation of a thinner film. As for EG3C7–C7, where the hydrocarbon component (C7–) possesses an equivalent number of hydrocarbon units (methyl/methylene) as the underlying alkyl part of the OEG-terminated component, both alkyl chain segments plausibly lie underneath the OEG moieties. Based on the Harder et al. model, the OEG portion has a large molecular cross section of  $21.3 \text{ \AA}^2$  and would be accommodated on top of a typical hydrocarbon layer, with a packing density of  $21.4 \text{ \AA}^2/\text{thiolate}$ .<sup>17</sup> The additional hydrocarbon chain underneath the OEG moieties probably provides a significant contribution to the decreased OEG-chain density on the surface, leading to an increase in chain tilt to enhance their lateral interactions, and giving rise to the observed low film thickness.

When the equilibrating temperature was increased, the film thicknesses of the double-chained dithiol SAMs decreased, as shown in [Figure 2](#). This phenomenon might be attributed to the formation of more disordered, loosely packed SAMs with an increased chain tilt in the structure. The thicknesses obtained from SAMs generated from each solvent were similar, indicating minimal solvent impact. However, the EG3C7–C7 SAM derived from DMF was exceptionally thin and probably corresponded to a poorly formed and highly disordered film.

We also determined the thicknesses of the films by evaluating the intensities of the C 1s and Au 4f peaks in the X-ray



**Figure 3.** Advancing contact angle ( $\theta_a$ ) data for water on the films generated from each adsorbate under designated conditions: C18SH, EtOH, room temperature; EG3C7SH, EtOH/DMF/THF, room temperature; EG3C7-C7 and EG3C7-C18, EtOH/DMF/THF, room temperature (23 °C) and at an elevated temperature (50 °C). Values were reproducible to  $\pm 2^\circ$ .

photoelectron spectra. Detailed procedures for these calculations and the corresponding results are described in the [Supporting Information](#) (see Table S2). Importantly, the calculated film thicknesses agree well with the ellipsometric film thicknesses (i.e., within  $\pm 2 \text{ \AA}$ ).

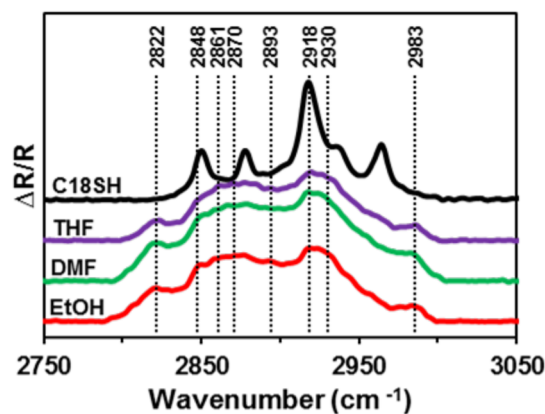
**Wettabilities of the Films.** The advancing contact angles on the surfaces of the SAMs generated from each adsorbate were collected using water and hexadecane as probe liquids. However, only water gave measurable contact angle values for the OEG-terminated SAMs generated from both monothiol and dithiol adsorbates; therefore, only the advancing contact angle data ( $\theta_a$ ) for water are shown in [Figure 3](#). The average contact angle for water obtained from the EG3C7SH SAM was consistent with the value obtained in a previous study of the methoxy-terminated tri(ethylene glycol) end group (i.e.,  $63^\circ \pm 2^\circ$ ).<sup>17</sup> These data indicate that the OEG-terminated SAMs are considerably less hydrophobic (i.e., lower  $\theta_a$ ) than the corresponding hydrocarbon SAM. The exposure of the glycol units at the outer surface allows the ether oxygen atoms to be accessible to water (i.e., increased interaction via hydrogen bonds)<sup>40</sup> and thus creates hydrophilic surfaces with low water contact angles.

Examining the data for the double-chained dithiol SAMs, the EG3C7-C18 SAM was less wettable than EG3C7SH SAM due to the exposure of hydrocarbon units in combination with the glycol units at the interface. On the other hand, the contact angle of water on the EG3C7-C7 SAM was similar to that on the EG3C7SH SAM, which would correspond to the exposure of only glycol units at the interfaces, regardless of the orientation of the glycol units (i.e., chain tilt), according to the thickness data obtained for these films. However, we must note that a decrease in the SAM thickness can be accompanied by an increase in the surface energy due to an increase in the influence of the van der Waals forces of the underlying gold.<sup>41</sup> Therefore, a small contact angle might be obtained for a thin film that reflects the underlying attractive interactions (e.g., van der Waals forces) between the metallic substrates and the liquids (through the SAMs), leading to a significant impact on the measured contact angles.<sup>42</sup> This phenomenon perhaps contributes to the similarity in the measured contact angles for water on the EG3C7-C7 SAMs generated from DMF as compared to those formed with other solvents, despite the differences in film thicknesses and/or film structures.

When the dithiol films were equilibrated during monolayer formation at an elevated temperature, the wettabilities increased. These data are consistent with the thickness

measurements and suggest that the films generated at a higher temperature were more disordered and less densely packed, which allowed for more oxygen atoms to be exposed at the surface, leading to enhanced film wettabilities. The van der Waals forces between the metallic substrates and the liquids probably also leads to reduced contact angle values for these thin films.<sup>42</sup>

**Characterization Using PM-IRRAS.** The surface IR spectra in the C–H stretching region for the EG3C7SH SAMs on gold are provided in [Figure 4](#). The position of the antisymmetric



**Figure 4.** PM-IRRAS of the EG3C7SH SAMs generated from EtOH, DMF, or THF at room temperature (23 °C) as compared to the spectrum of the C18SH SAM.

( $\nu_{\text{as}}^{\text{CH}_2}$ ) and symmetric ( $\nu_{\text{s}}^{\text{CH}_2}$ ) methylene C–H stretching bands at 2918 and 2849  $\text{cm}^{-1}$ , respectively, are the same as those found for conformationally ordered *n*-alkanethiolate SAMs on gold,<sup>43–45</sup> but we caution that the broadness of the peaks observed in [Figure 4](#) allows us to draw no conclusions regarding the chain conformations in the EG3C7SH SAMs. [Table 1](#) shows the assignments of each of the IR bands associated with the ethylene glycol (EG) moieties observed in crystalline PEG, amorphous PEG, and OEG-terminated surfaces, data that have been previously reported.<sup>17,36</sup> The methyl C–H stretching bands ( $\nu_{\text{as}}^{\text{CH}_3}$  at 2964  $\text{cm}^{-1}$ ;  $\nu_{\text{s}}^{\text{CH}_3}$  at 2878  $\text{cm}^{-1}$ ) and the associated Fermi resonance band (2938  $\text{cm}^{-1}$ )<sup>43</sup> typically found for the termini of alkyl chains are absent from the spectra. Instead, the methyl C–H stretching bands generally associated with such glycol moieties are present at 2983 and 2822  $\text{cm}^{-1}$ , suggesting the existence of terminal methoxy groups on the surfaces. Two bands at 2893 and 2861

**Table 1. Assignment of the Peaks in the IR Spectral Region Associated with the C–H Stretching Vibrations for the Ethylene Glycol Units (–OCH<sub>2</sub>CH<sub>2</sub>–)**

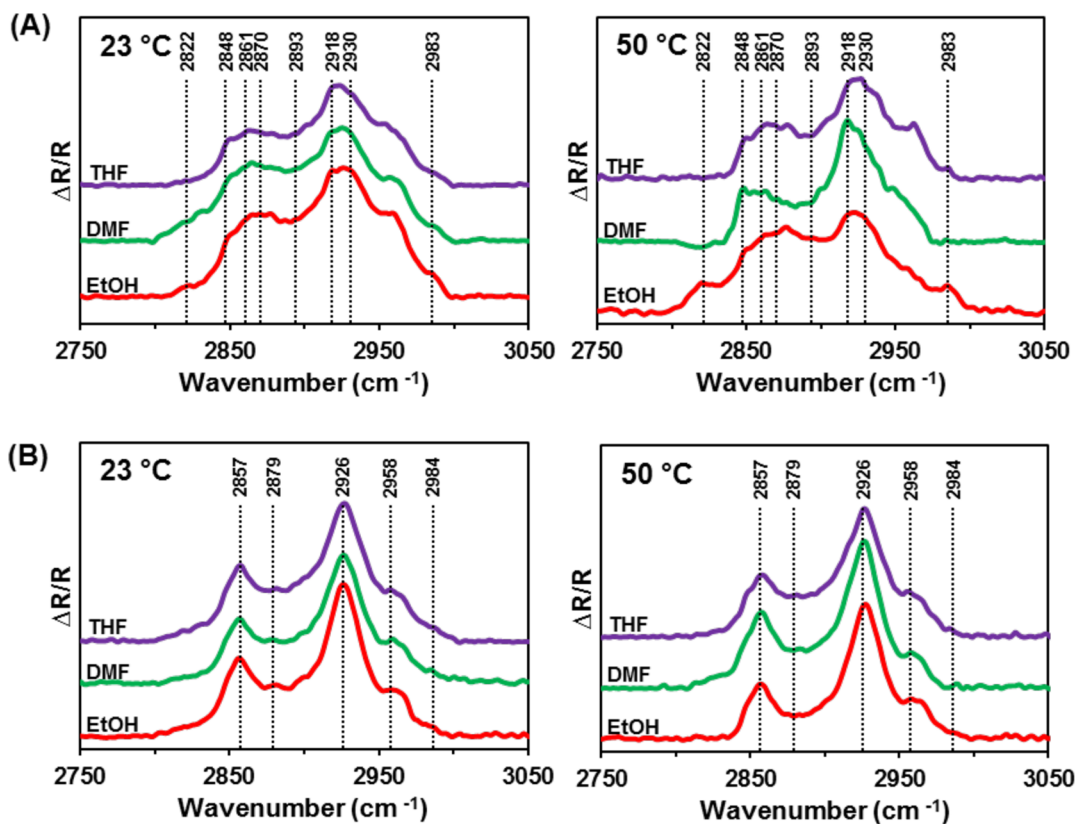
mode	polarization <sup>a</sup>	PEG, crystalline	PEG, amorphous	EG3-OMe/Au <sup>b</sup>
EG CH <sub>3</sub> asym				2982
EG CH <sub>3</sub> sym				2819
EG CH <sub>2</sub> asym	⊥	2950	2930	2930
EG CH <sub>2</sub> sym	∥	2890	2865	2894
	⊥	2885		2870
	∥	2865		2861
EG combination	∥	2740	2740	2740
alkyl CH <sub>2</sub> asym				2919
alkyl CH <sub>2</sub> sym				2853

<sup>a</sup>Transition dipole moment with respect to the helical axis in crystalline PEG. <sup>b</sup>Previously reported OEG-terminated alkanethiolate SAM on gold.<sup>17</sup>

cm<sup>-1</sup> can be assigned to the symmetric methylene C–H stretching modes of the crystalline helical OEG moieties. Another methylene C–H stretching band at 2870 cm<sup>-1</sup> with a shoulder at 2930 cm<sup>-1</sup>, characteristic for gauche conformations, is also shown in the spectra. As a result, we conclude that the molecular conformation of the OEG moieties in the EG3C7SH SAMs conform with that of crystalline helices coexisting with amorphous conformers.<sup>17,36</sup> The helical structure is a key factor in the protein resistance of this hydrophilic film, an aspect of this study that is discussed in a later section.

Figure 5A shows the PM-IRRAS spectra of the EG3C7–C7 SAMs generated under a variety of conditions. These spectra are comparable to those of EG3C7SH shown in Figure 4, indicating the presence of an underlying alkyl segment and an OEG terminus. The inclusion of a hydrocarbon chain in the double-chained structure of this adsorbate contributed to the additional bands at 2962 and 2876 cm<sup>-1</sup> for the methyl C–H stretching vibrations and an enhancement in the  $\nu_{\text{as}}^{\text{CH}_2}$  band (2918 cm<sup>-1</sup>) intensity; however, the further broadening of this band due to overlap with the peak associated with  $\nu_{\text{as}}^{\text{CH}_2}$  of the OEG ethylene moieties prohibits our use these spectra to discern the conformational ordering of the alkyl chains within the EG3C7–C7 films.<sup>46</sup> By contrast, the IR spectra of the EG3C7–C18 SAMs provided in Figure 5B show that the band positions of the methylene C–H stretching vibrations were shifted to higher wavenumbers (2926 and 2858 cm<sup>-1</sup> for  $\nu_{\text{s}}^{\text{CH}_2}$  and  $\nu_{\text{s}}^{\text{CH}_3}$ , respectively), consistent with the presence of liquid-like conformations for the hydrocarbon chains owing to the strong influence of the OEG moieties upon the ordering of these chains.<sup>45</sup> Other peak assignments within the C–H stretching region of the IR spectra for the OEG moieties proved ambiguous due to an overlap of the glycol bands with the intense CH<sub>2</sub> stretching bands.

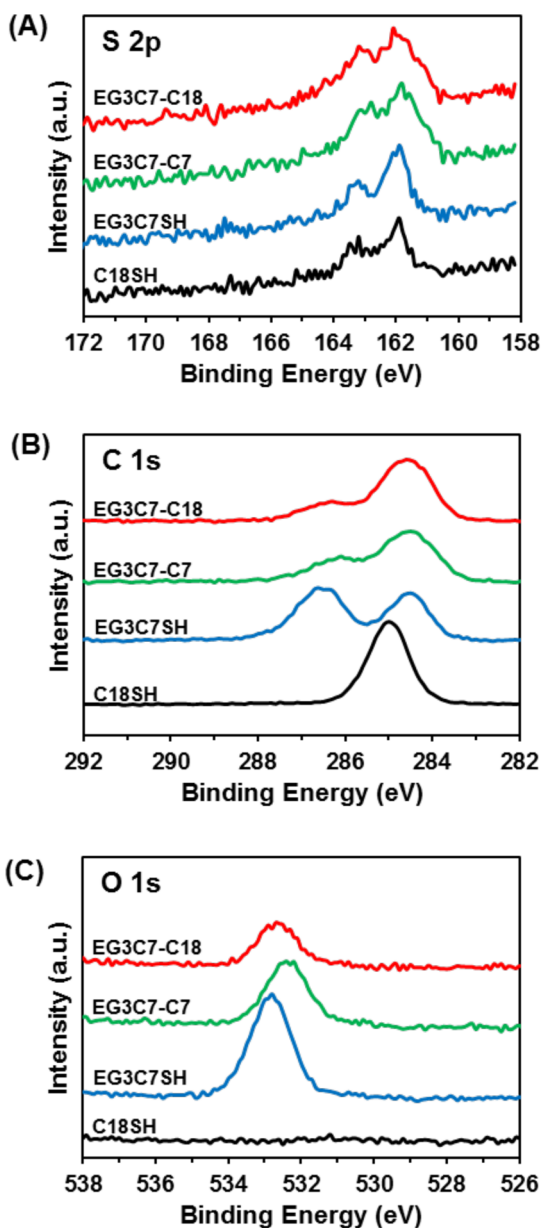
**Characterization Using XPS.** X-ray photoelectron spectroscopy (XPS) is a spectroscopic technique used to determine the elemental composition of materials, including organic thin films.<sup>47,48</sup> In the X-ray photoelectron spectra, the displayed binding energy (BE) of each elemental component depends in part upon the electron density of a particular atom and is sensitive to its oxidation state and its interactions with the surrounding atoms. In the case of multidentate alkanethiolate



**Figure 5.** PM-IRRAS spectra for SAMs formed from (A) EG3C7–C7 and (B) EG3C7–C18 generated from EtOH, DMF, or THF at room temperature (23 °C) and an elevated temperature (50 °C).

SAMs on gold, the BEs of the S 2p peaks (a doublet comprised of S 2p<sub>3/2</sub> and S 2p<sub>1/2</sub> in a 2:1 area ratio with a splitting of 1.2 eV) can be used to determine the nature of the bonding of the adsorbate to the surface.<sup>48</sup> For the S 2p<sub>3/2</sub> peak for unbound thiols or disulfides, the BE peak will appear at ~163.5–164 eV, whereas the BE of the thiolate species bonded on gold appears at ~162 eV. If the sulfur atoms are in highly oxidized states, the S 2p<sub>3/2</sub> peak will exhibit at a BE greater than 166 eV.<sup>49</sup>

The X-ray photoelectron spectra of SAMs generated from EG3C7–C7 and EG3C7–C18 in Figure 6 confirm the presence of sulfur, carbon, and oxygen atoms, as expected. Further, the S 2p spectra of the EG3C7–C7, and EG3C7–C18 SAMs exhibit only a doublet where the S 2p<sub>3/2</sub> peak is located at ~162 eV, confirming complete S–Au bond formation for both sulfur headgroups in each adsorbate and the chelating



**Figure 6.** High-resolution X-ray photoelectron spectra of the (A) S 2p, (B) C 1s, and (C) O 1s regions of the EG3C7–C18, EG3C7–C7, EG3C7SH, and C18SH SAMs generated from EtOH at room temperature (23 °C).

character of the resultant SAMs (Figure 6A). Additionally, the absence of peaks at 166 eV and above indicates that there were no oxidized sulfur species in any of the films. Furthermore, the percentages of bound thiolate were evaluated by deconvolution of the peaks in the S 2p region of the X-ray photoelectron spectra (see Figure S6 in the Supporting Information). The percentages of bound thiolate for EG3C7–C18, EG3C7–C18, EG3C7SH, and C18SH in EtOH at room temperature (23 °C) were 92, 89, 98, and 100%, respectively.

Figure 6B shows the C 1s photoelectron peaks obtained for each SAM. In the case of normal alkanethiolate SAMs, the C 1s BE peak centers at 285.0 eV and is attributed to the carbon atoms within the hydrocarbon backbone.<sup>19,50</sup> For all the OEG-terminated thiols, the comparable C 1s BE peaks (i.e., those associated with the underlying methylene chain) were shifted to lower binding energies at ~284.5 eV. Several studies have demonstrated the sensitivity of the binding energy of the C 1s peak to changes in the relative coverage (i.e., packing density) of adsorbates on the substrate; the explanation frequently offered for these shifts is that an electron emission from a loosely packed surface, which acts as a poor insulator, produces positive charges that are more readily discharged, which can cause the C 1s peak to shift to a lower binding energy.<sup>19,50–54</sup> Accordingly, we can see that the OEG moieties incorporated in the monolayers contributed to a decrease in hydrocarbon chain density, causing the formation of a less densely packed SAM as compared to the normal alkanethiolate film. The C 1s peak observed at approximately 286.6 eV represents the ejection of the photoelectrons from the ether carbon atoms (C–O–C) of the glycol unit, where carbon atoms are directly attached to the more electronegative oxygen atom, making these carbon atoms electron deficient, giving rise to an increase in the C 1s binding energy.<sup>47,55</sup> The differences in the relative intensities of the C–O–C/CH<sub>2</sub> C 1s peaks among the EG3C7SH, EG3C7–C7, and EG3C7–C18 spectra correspond to the molecular composition of each film (i.e., the number of carbons in the methylene chain segments vs those in the glycol units), and to the relative position of these moieties within the film (i.e., the influence of attenuation).

Additional evidence supporting the presence of the glycol group within the SAM assembly can be observed in the XPS spectral region containing the O 1s peak, as shown in Figure 6C. This peak, which is representative of glycol oxygen, is centered at ~532.8 eV for the EG3C7SH film.<sup>56</sup> For the O 1s peaks observed in the dithiolate SAMs, ~532.4 eV for the EG3C7–C7 SAMs and ~532.6 eV for the EG3C7–C18 SAMs, the shifts to lower BEs occurred as the relative concentration of the OEG phase, as compared to the hydrocarbon phase, decreased (i.e., having additional hydrocarbon chain in the structure as compared to the EG3C7SH SAM). The observed shifts appear to correlate with the OEG chain densities in the monolayers when the films composed of the double-chained structure are loosely packed, as judged by the positions of the C 1s (C–O–C) peaks mentioned above, and probably indicate a decrease in terminal OEG chain densities on the surfaces. The X-ray photoelectron spectra for the EG3C7–C7 and EG3C7–C18 monolayers prepared under other conditions were also collected (data not shown) and showed similar spectral components to those of the SAMs derived from EG3C7–C7 and EG3C7–C18 in Figure 6. These data, therefore, provided no additional insight regarding the structure and/or packing of the SAMs formed under the various conditions.

**Table 2.** Comparison of the Ellipsometric Film Thicknesses, the XPS-Derived Carbon-to-Gold (C/Au), Oxygen-to-Gold (O/Au), and Sulfur-to-Gold (S/Au) Ratios, the Relative Chain Packing Densities, and Contact Angle Measurements for Films Generated from C7SH, C18SH, EG3C7SH, EG3C7SH/C7SH, EG3C7–C7, EG3C7SH/C18SH, and EG3C7–C18 at Room Temperature (23 °C) in EtOH

	C7SH	C18SH	EG3C7SH	EG3C7SH/C7SH	EG3C7–C7	EG3C7SH/C18SH	EG3C7–C18
C/Au	0.0366	0.1518	0.0717	0.0479	0.0506	0.1458	0.0811
O/Au	0.0000	0.0000	0.0676	0.0171	0.0169	0.0000	0.0168
S/Au	0.0045	0.0073	0.0064	0.0069	0.0068	0.0071	0.0063
relative chain packing density <sup>a</sup>	0.62	1.00	0.88	0.95	0.93	0.97	0.86
ellipsometric film thickness <sup>b</sup>	9 Å	21 Å	15 Å	10 Å	10 Å	22 Å	11 Å
contact angles of water ( $\theta_a$ ) <sup>b</sup>	105°	115°	65°	71°	66°	110°	83°

<sup>a</sup>The S/Au ratio for the C18SH SAM (0.0073) was used to produce relative chain packing densities for the films, assuming the packing density of the C18SH film to be 100%. <sup>b</sup>Ellipsometric thickness and contact angle measurement reproducibilities were within  $\pm 2$  Å and  $\pm 2^\circ$ , respectively. These data are the average of multiple measurements, as further detailed in the Supporting Information, and were collected during examination of the mixed-SAMs independently from the data collected and presented in Table S1, Figure 2, and Figure 3.

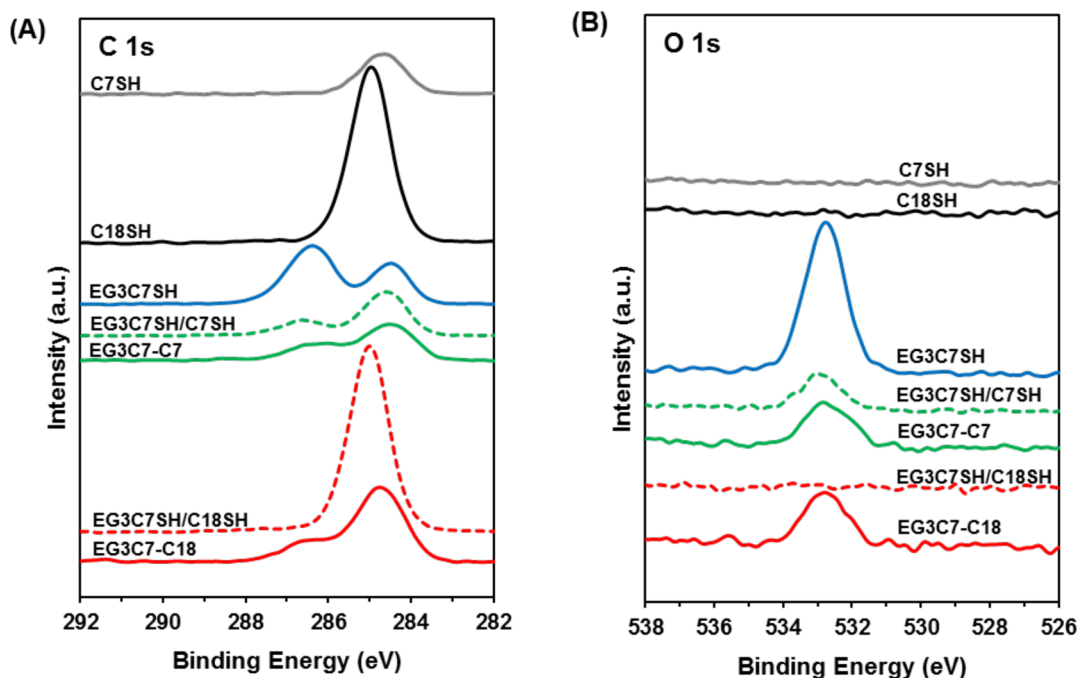
One additional means of using XPS to analyze self-assembled thin films formed from thiolate adsorbates is to examine the S 2p/Au 4f ratios derived from the integrated areas under their respective peaks in the X-ray photoelectron spectra. Table 2 provides these data along with the composite peak intensity ratios for C 1s/Au 4f and O 1s/Au 4f for each of the SAMs prepared for this study. Prior work involving monolayer films has demonstrated that such ratios can be useful in determining the relative packing characteristics of the adsorbates on the surface of gold.<sup>28</sup> For our analysis of the SAMs, we used the S/Au ratios to provide an understanding of the relative packing densities of the alkyl/OEG chains, recognizing that there is an equivalent number of overlying chains for each sulfur headgroup in the adsorbates. Consideration must be given, however, to factors that might skew the collected data, such as the influence of the relative thicknesses of the films, owing to attenuation of the XPS signals. For our SAMs, the relatively small signal for sulfur is likely impacted to a different degree than that of gold because the decay in the XPS signal is an exponential function that depends on the overlying film thickness. For the four films in question, C18SH, EG3C7SH, EG3C7–C7, and EG3C7–C18, the average film thicknesses are 21, 15, 10, and 11 Å, respectively; consequently, it is plausible that the differences in the thicknesses of the monolayer chain assemblies might skew the collected S/Au ratios, limiting their usefulness as a tool for comparison. To investigate this concern, we collected S/Au ratios for a series of alkanethiolate films formed from C8SH, C10SH, C12SH, C14SH, C16SH, and C18SH and compared these data with those from other alkanethiolate SAMs obtained from several recent publications (see Figure S5 in the Supporting Information). From our analysis of these data, we conclude that, within the limited range of film thicknesses examined in Figure S5 (a range inclusive of the film thicknesses found in this study), the associated S/Au ratios for SAMs of similar packing characteristics will either be statistically invariant or exhibit a slight increase in value with increasing film thickness.

Using the XPS S/Au ratio for the C18SH SAM to provide a means of defining a monolayer with 100% packing, we produced a relative chain packing density parameter to enable facile comparison of the data for our analysis of the monolayer films, as shown in Table 2. Based on the resulting values, the general order for the relative chain packing densities for our SAMs is as follows: C18SH > EG3C7–C7 > EG3C7SH  $\cong$  EG3C7–C18. Since there appears to be no substantial influence of the film thicknesses skewing the data used to

obtain these results, the question becomes what factors contribute to the ordering of these SAMs with regard to the relative chain packing densities? For the C18SH SAM, the *trans*-extended alignment of the simple alkyl chains of this type of assembly allows for the formation of a tightly packed film, leading it to possess the highest relative chain packing density (1.00 for our relative chain packing density parameter). The adsorbate structure of the EG3C7–C7 SAM (0.93) enables these double-chained dithiols to pack with both C7 alkyl chain segments assembling below the overlying OEG moieties; therefore, the more bulky component of these adsorbates has more space to form an organized assembly, providing a rationale for this film packing more efficiently than the EG3C7SH SAM. By contrast, both the EG3C7SH (0.88) and EG3C7–C18 (0.86) SAMs must adopt headgroup bonding arrangements that allow sufficient space for the large molecular cross section of the OEG moieties.

Notably, the chain coverage of the SAM derived from EG3C7–C7 is slightly greater than that of the SAM derived from EG3C7SH, yet the former gives rise to a markedly thinner film. We propose that this difference arises, at least in part, from a relative absence of water in the EG3C7–C7 SAM compared to that in the EG3C7SH SAM.<sup>17</sup> A similar rationalization holds for the longer-chain EG3C7–C18 SAM, where the observed film thickness is concomitantly diminished by its lower chain packing density (i.e., only 86% for the EG3C7–C18 SAM).

**II. Comparison between Unsymmetrical Oligo-(ethylene glycol) Spiroalkanedithiolate-SAMs and Mixed-SAMs Formed from Adsorbates with Equivalent Chain Composition.** The valuable role of tying the two phase-incompatible chains into one adsorbate structure can best be demonstrated by comparing the unsymmetrical spiroalkanedithiolate SAMs (i.e., EG3C7–C18 and EG3C7–C7) to films formed from mixtures of adsorbates with chain compositions equivalent to those found in the dithiolate films (i.e., EG3C7SH/C18SH and EG3C7SH/C7SH). For simplicity, we refer to the comparison of the SAM formed from the dithiol EG3C7–C7 to the mixed SAM formed from the monothiol adsorbate pair EG3C7SH/C7SH as the C7 films, while the SAM formed from the dithiol EG3C7–C18 compared to the mixed SAM formed from the monothiol adsorbate pair EG3C7SH/C18SH encompass the C18 films. For this aspect of our report, we have relied upon ellipsometry, contact angle goniometry, and X-ray photoelectron spectroscopy to make determinations regarding how these two



**Figure 7.** High-resolution XPS spectra of the (A) C 1s and (B) O 1s regions of the C7SH, C18SH, EG3C7SH, EG3C7SH/C7SH, EG3C7-C7, EG3C7SH/C18SH, and EG3C7-C18 SAMs generated from EtOH at room temperature (23 °C).

approaches to mixed-film assembly impact the properties of the resulting films.

**Thicknesses of the Mixed Films.** As shown in Table 2, the C7 films exhibited equivalent thicknesses of 10 Å each, while the C18 films were totally dissimilar: the EG3C7-C18 dithiolate SAM had a thickness of 11 Å, while the EG3C7SH/C18SH SAM had a thickness of 22 Å. For the latter, these results might indicate that the mixture of adsorbates in the film is dominated by the C18SH adsorbate, whose single-component SAM exhibited a thickness of 21 Å.

**Wettabilities of the Mixed Films.** Regarding the wettability of the SAMs using water as the contacting liquid, the C7 films again produced similar results, while the C18 films were dissimilar. For the EG3C7-C7 dithiolate SAM, the water contact angle was 66°, while that for the analogous mixed SAM was 71°. This difference in the measured contact angles might indicate the contacting liquid is intercalating in the chains of the EG3C7SH/C7SH mixed SAM more than in the chains of the dithiolate SAM. Such a conclusion is plausible, particularly considering that the contact angle for water on the SAM formed from EG3C7SH is statistically the same as that on the relatively well-packed EG3C7-C7 SAM (*vide supra*). Alternatively, the minor variance in the contact angle measurements between the two C7 films might reflect a failure for the binary adsorbate system to produce monolayers in which the two types of chains are intimately mixed, instead producing two-dimensional structures where the two components form nano- or microscale domains. In contrast, for the C18 films, the SAM formed from the EG3C7SH/C18SH adsorbate pair produced an average contact angle of 110°, almost equal to the 115° for the C18SH SAM, while the EG3C7-C18 dithiolate SAM generated an average measurement of 83°, a number that appears to align with the anticipated blending of the two component chains present in this monolayer.

**Characterization of the Mixed Films Using XPS.** The X-ray photoelectron spectra provide further support for the

divergence in the characteristics of the C7 films and C18 films. The data in Table 2 show that the EG3C7SH/C7SH mixed SAM and the EG3C7-C7 dithiolate SAM produced films with similar chain packing characteristics, but to our surprise, the mixed SAM yielded the higher relative chain packing density (0.95 versus 0.93). This result might indicate favorable film formation dynamics associated with this pair of adsorbates, where both structures allow the alkyl chain segments to assemble under the overlying OEG termini. These results are in stark contrast to those of the EG3C7SH/C18SH mixed SAM and the EG3C7-C18 dithiolate SAM. For the latter, the relative chain packing density of 0.86 indicates that the packing of the thiolate headgroups is less than that for all the other films with OEG termini, as noted above in the analysis of the relative packing characteristics of the films produced in this study. Yet for the EG3C7SH/C18SH mixed SAM, the relative chain packing density is 0.97, a number that aligns closely with that of the SAM formed from C18SH.

Further support for a conclusion that the mixed SAM formed from the EG3C7SH/C18SH adsorbate pair has more in common with the C18SH SAM can be found in the C/Au ratios in Table 2, where the ratio for the C18SH SAM (0.1518) is similar to that of the EG3C7SH/C18SH mixed SAM (0.1458), but not that of the EG3C7-C18 dithiolate SAM (0.0811), as can be observed in the spectra in Figure 7. Additionally, the EG3C7SH/C18SH mixed SAM failed to produce a measurable O/Au ratio, leaving in doubt whether this particular SAM incorporates any measurable amount of the EG3C7SH component. As for the EG3C7SH/C7SH mixed SAM and the EG3C7-C7 dithiolate SAM, the C/Au ratios (0.0479 and 0.0506, respectively) and the O/Au ratios (0.0171 and 0.0169, respectively) were similar, consistent with a model in which the composition of these two films are similar.

**III. Thermal Stability of OEG-Terminated SAMs on Evaporated Gold Surfaces.** One of the benefits frequently associated with SAMs formed from bidentate adsorbates is a



substantial improvement in the stability of the resulting films.<sup>27–29</sup> To evaluate the thermal stability of the SAMs developed from EG3C7SH, EG3C7–C7 and EG3C7–C18 in EtOH, we performed solution-phase thermal desorption tests analogous to those detailed previously.<sup>28</sup> We used ellipsometric thickness measurements to determine the average amount of adsorbate remaining after prolonged heating at either 70 or 90 °C in a large excess of the nonpolar solvent decahydronaphthalene (decalin). Thickness measurements were acquired in 10 min intervals for 1 h. The resulting data were compiled in the two plots displayed in Figure 8, which revealed substantial

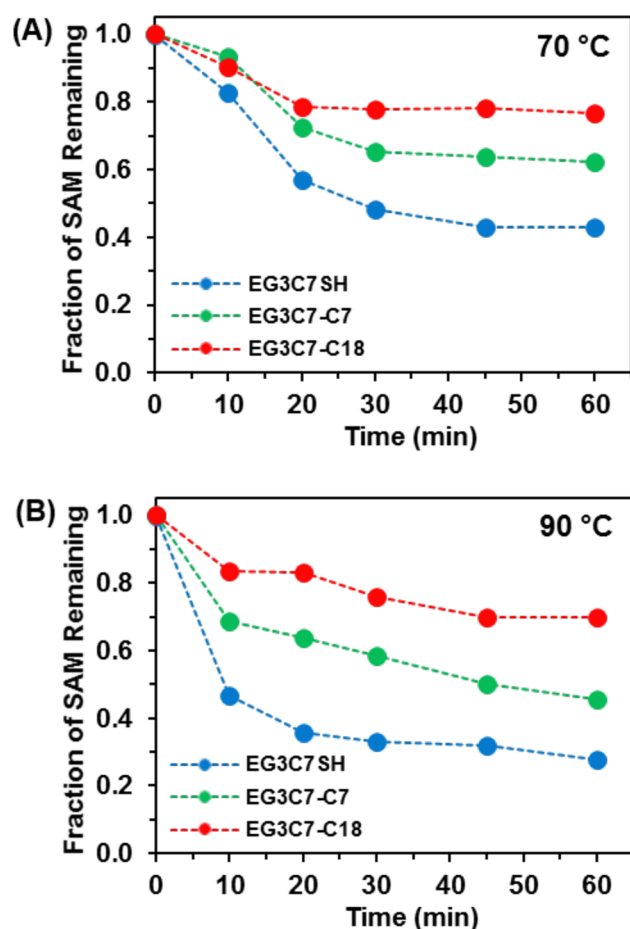


Figure 8. Solution-phase thermal desorption profiles of the indicated SAMs in decalin at (A) 70 °C and (B) 90 °C.

differences in thermal stability between the two dithiolate films. Under conditions in which a low level of heat was applied (70 °C, Figure 8A), ~80% of the EG3C7–C18 and ~60% of the EG3C7–C7 adsorbates remained on the surface after 60 min, but less than 40% of the EG3C7SH SAM remained under the same conditions. At a slightly higher temperature (90 °C, Figure 8B), ~70% of the EG3C7–C18 adsorbates remained on the surface after 60 min. Under the same conditions, the fraction of the EG3C7–C7 adsorbates remaining on the surface (~50%) was substantially less than that of the EG3C7–C18 SAM. However, the EG3C7–C18 and EG3C7–C7 films still proved to be markedly more stable than the EG3C7SH film at the higher temperature (90 °C). These results can be interpreted to indicate that the bidentate nature of the spiroalkanedithiol headgroup plays an important role in enhancing thermal stability. The greater stability of SAMs

derived from EG3C7–C18 compared to those derived from EG3C7–C7 suggests that interchain van der Waals interactions play an important role in stabilizing the EG3C7–C18 films relative the EG3C7–C7 films.<sup>19</sup>

**IV. Preliminary Studies of Protein Adsorption.** To perform our protein adsorption study, the new OEG-terminated dithiolate SAMs were generated under various conditions, along with monothiolate SAMs formed from a normal alkanethiol and an OEG-terminated alkanethiol. Such comparisons provide an opportunity to determine the relative contribution to the thin-film properties for the SAMs formed from EG3C7–C7 and EG3C7–C18 from the alkyl and OEG components that correspond to the C18SH and EG3C7SH adsorbates, respectively. This aspect of the analysis is particularly important because of the differences in adhesive character toward protein for the two types of monolayers; OEG-terminated films exhibit antiadhesive character while hydrocarbon-terminated films are more adhesive.<sup>22</sup> In this brief study, we examined the protein resistance of the new OEG-terminated double-chained dithiolate SAMs using fibrinogen as a model protein. The amount of fibrinogen adsorption from a PBS buffer solution onto the monolayers was estimated by ellipsometry, and the data are shown in Table 3. All data were

Table 3. Amount of Fibrinogen Adsorption (%) on SAMs Derived from the Monothiolate Adsorbates C18SH and EG3C7SH at Room Temperature and Bidentate Dithiolate Adsorbates EG3C7–C7 and EG3C7–C18 at Room Temperature (23 °C) and an Elevated Temperature (50 °C) Using Several Solvents

	C18SH	EG3C7SH	EG3C7–C7		EG3C7–C18	
			23 °C	50 °C	23 °C	50 °C
EtOH	100 <sup>a</sup>	0	77	77	68	67
DMF	-- <sup>b</sup>	0	67	64	64	68
THF	--	0	65	65	67	68

<sup>a</sup>All data were normalized to the amount of fibrinogen adsorption on the C18SH film. <sup>b</sup>The C18SH SAM was only prepared at room temperature using ethanol as the equilibrating solvent.

normalized to the amount of fibrinogen adsorption on the film formed from C18SH, which was considered to have no ability to resist the adsorption of protein (100% adsorption). The EG3C7SH SAM with the helical conformation of the terminal OEG chains, as probed by IR, showed an excellent ability to suppress protein adhesion on the surface, a result that is consistent with work done by Whitesides and co-workers,<sup>13,17</sup> who found that the OEG-terminated alkanethiol SAM on gold with the helical form of the OEG units was protein resistant, whereas the all-*trans* planar form of OEG components of this film on silver adsorbed protein.

The mechanisms involved in the inhibition of protein adsorption on PEG surfaces are not completely understood; nevertheless, the phenomenon can be rationalized through previous theoretical studies. It has been proposed that the approach of protein molecules to the surface initiates the compression of PEG chains, which reduces the degree of conformational freedom on the interface and thus leads to an entropic repulsion between the surface and the macromolecules (i.e., a steric repulsion effect).<sup>2,57</sup> On the other hand, Szeifer proposed that a dense PEG monolayer can block contact between protein and the hydrophobic substrate better than a flexible PEG monolayer.<sup>58</sup> Furthermore, the presence of a

stable water layer bound at the protein/SAM interface has also been proposed to exert a strong influence on protein resistance by preventing direct interaction between the surface and the protein and/or introducing a greater steric repulsion effect as the protein approaches the surface; it is also important to note that the OEG moieties are strongly solvated by water, which conveys a substantial enthalpic cost when the protein displaces bound water, and a consequent reduction in the thermodynamic driving for adsorption.<sup>17,59,60</sup> The latter can be related to the molecular conformation of OEG moieties on the surface, where the helical structure easily accommodates water molecules (due to the strong dipole moment of water) while the denser all-*trans* conformation prevents water from penetrating the film and forming strong interactions within the film.<sup>40</sup> Consequently, the helical OEG-terminated SAM can resist protein adsorption better than the OEG-terminated SAM with the *trans*-extended planar conformation.<sup>17,40</sup> In the case of the SAMs derived from the double-chained dithiolates, EG3C7-C7 and EG3C7-C18, the ability to resist protein adsorption was comparable for all SAMs examined despite differences in adsorbate structures and the conditions used to prepare the samples. In addition, the double-chained OEG-functionalized SAMs showed no great ability to resist protein adsorption. This phenomenon might be attributed to the presence of alkyl chains at the interface, which (i) reduce the binding of interfacial water within the film leading to greater interactions between the proteins and the surfaces and/or (ii) the alkyl chains directly contacting the protein molecules. Nevertheless, the measured contact angles of water showed no correlation with these possible explanations, which likely eliminates the surface energy of our SAM interfaces as the root cause for the observed protein adhesion to the bidentate SAMs. Nevertheless, the combination of an increased presence of hydrophobic chains, along with a reduced ordering for the hydrophilic chains, reduces the intermolecular strength of the network of adsorbed water. These circumstances therefore would allow improved access and adhesion by proteins to the SAM interface—a possible rationalization for our results that aligns with that previously proposed by Harder et al.<sup>17</sup>

## CONCLUSIONS

The unsymmetrical oligo(ethylene glycol) spiroalkanedithiol adsorbates, EG3C7-C7 and EG3C7-C18, were synthesized and used to generate SAMs on gold under varying conditions (equilibrating solvents and temperatures). These SAMs were characterized using ellipsometry, contact angle goniometry, surface IR spectroscopy, and XPS, with the resulting data being compared with the SAMs formed from the normal alkanethiol (C18SH) and OEG-terminated alkanethiol (EG3C7SH) analogues. We believe that the low film thicknesses of the double-chained dithiolate SAMs arise from the presence of the additional hydrocarbon chain in combination with the phase-incompatible OEG moiety, which contributes to disorder in the films and/or an increase in chain tilt. The comparable wettabilities of the EG3C7SH and EG3C7-C7 SAMs indicate the exposure of the OEG moieties at both interfaces, whereas the less wettable (i.e., less hydrophilic) EG3C7-C18 SAM corresponds to the exposure of hydrocarbon units at the interface. XPS data confirmed the formation of these new OEG-terminated dithiolate SAMs having less densely packed structures owing to the relatively large molecular cross sections for the OEG moieties and the double-chained nature of the adsorbates.

Comparisons to offsetting mixed SAMs formed from monothiol pairs of analogous chain compositions to the two halves of the dithiol structures produced SAMs which both aligned with (i.e., the SAM formed from the EG3C7SH/C7SH pair compared to the EG3C7-C7 SAM) and diverged from (i.e., the SAM formed from the EG3C7SH/C18SH pair compared to the EG3C7-C18 SAM) the characteristics of our new spiroalkanedithiolate SAMs. In particular, the C7 films yielded almost identical characterization data, revealing the favorable film formation dynamics for the pair of adsorbates where both structures allow the alkyl chain segments to assemble under the overlying OEG termini. For the C18 films, the differences in the collected data pointed to the failure of the EG3C7SH component of the mixed film to surface adsorb and contribute, to any measurable extent, to the characteristics of the resulting SAM. This aspect of our study reveals that there are some mixed-SAM compositions that are only accessible through the intimate blending of the phase-incompatible components within a single adsorbate structure. A thermal stability study conducted in a nonpolar solvent revealed that the organic thin-films derived from EG3C7-C7 and EG3C7-C18 are markedly more stable than those derived from EG3C7-C7 when heated to both 70 and 90 °C. These OEG-terminated adsorbates also possess four features commonly found in surfaces that resist the adsorption and adhesion of proteins (and other biological species): (1) high polarity, (2) the absence of hydrogen-bond donors, (3) the presence of hydrogen-bond acceptors, and (4) a charge-neutral contact surface.<sup>58</sup> In our brief study of protein adsorption, the mixed SAMs formed from an intimate combination of hydrocarbon and OEG-components showed a greater ability to resist the adsorption of fibrinogen on their surfaces when compared to the C18SH film, but not better than the EG3C7SH films. From the data, we conclude that it is likely that the presence of the hydrophobic alkyl chain led to the observed reduction in protein resistance for the EG3C7-C7 and EG3C7-C18 SAMs.

## ASSOCIATED CONTENT

### Supporting Information

The Supporting Information is available free of charge on the ACS Publications website at DOI: 10.1021/acs.langmuir.6b03803.

Detailed descriptions of the materials and synthetic procedures for preparing 2,5,8,11-tetraoxaocadecane-18-thiol (EG3C7SH), 2-(2,5,8,11-tetra-oxahexadecan-16-yl)-2-pentylpropane-1,3-dithiol (EG3C7-C7), and 2-(2,5,8,11-tetraoxahexadecan-16-yl)-2-hexadecylpropane-1,3-dithiol (EG3C7-C18), along with <sup>1</sup>H and <sup>13</sup>C NMR, the instrumental and experimental procedures used to conduct this research, and supplementary data. (PDF)

## AUTHOR INFORMATION

### Corresponding Author

\*E-mail: trlee@uh.edu.

### ORCID

T. Randall Lee: 0000-0001-9584-8861

### Notes

The authors declare no competing financial interest.

## ACKNOWLEDGMENTS

We thank the National Science Foundation (CHE-1411265), the Robert A. Welch Foundation (Grant No. E-1320), and the Texas Center for Superconductivity at the University of Houston for generous support.

## REFERENCES

- (1) Harris, J. M.; Zalipsky, S. *Poly(ethylene glycol) Chemistry and Biological Applications*; American Chemical Society: Washington, DC, 1997.
- (2) Jeon, S. I.; Andrade, J. D. Protein-Surface Interactions in the Presence of Polyethylene Oxide. II. Effect of Protein Size. *J. Colloid Interface Sci.* **1991**, *142*, 159–166.
- (3) Taunton, H. J.; Toprakcioglu, C.; Fetters, L. J.; Klein, J. Forces between Surfaces Bearing Terminally Anchored Polymer Chains in Good Solvents. *Nature* **1988**, *332*, 712–714.
- (4) Banerjee, I.; Pangule, R. C.; Kane, R. S. Antifouling Coatings: Recent Developments in the Design of Surfaces That Prevent Fouling by Proteins, Bacteria, and Marine Organisms. *Adv. Mater.* **2011**, *23*, 690–718.
- (5) Yang, W.; Hamers, R. J. Fabrication and Characterization of a Biologically Sensitive Field-effect Transistor Using a Nanocrystalline Diamond Thin Film. *Appl. Phys. Lett.* **2004**, *85*, 3626–3628.
- (6) Zhang, F.; Kang, E. T.; Neoh, K. G.; Huang, W. Modification of Gold Surface by Grafting of Poly(ethylene glycol) for Reduction in Protein Adsorption and Platelet Adhesion. *J. Biomater. Sci., Polym. Ed.* **2001**, *12*, 515–531.
- (7) Castner, D. G.; Ratner, B. D. Biomedical Surface Science: Foundations to Frontiers. *Surf. Sci.* **2002**, *500*, 28–60.
- (8) Ko, B. S.; Babcock, B.; Jennings, G. K.; Tilden, S. G.; Peterson, R. R.; Cliffl, D.; Greenbaum, E. Effect of Surface Composition on the Adsorption of Photosystem I onto Alkanethiolate Self-Assembled Monolayers on Gold. *Langmuir* **2004**, *20*, 4033–4038.
- (9) Lahiri, J.; Kalal, P.; Frutos, A. G.; Jonas, S. J.; Schaeffler, R. Method for Fabricating Supported Bilayer Lipid Membranes on Gold. *Langmuir* **2000**, *16*, 7805–7810.
- (10) Jenkins, A. T. A.; Bushby, R. J.; Evans, S. D.; Knoll, W.; Offenhausser, A.; Ogier, S. D. Lipid Vesicle Fusion on  $\mu$ CP Patterned Self-Assembled Monolayers: Effect of Pattern Geometry on Bilayer Formation. *Langmuir* **2002**, *18*, 3176–3180.
- (11) Luk, Y.-Y.; Tingey, M. L.; Hall, D. J.; Israel, B. A.; Murphy, C. J.; Bertics, P. J.; Abbott, N. L. Using Liquid Crystals to Amplify Protein-Receptor Interactions: Design of Surfaces with Nanometer-Scale Topography that Present Histidine-Tagged Protein Receptors. *Langmuir* **2003**, *19*, 1671–1680.
- (12) Prime, K. L.; Whitesides, G. M. Self-Assembled Organic Monolayers: Model Systems for Studying Adsorption of Proteins at Surfaces. *Science* **1991**, *252*, 1164–1167.
- (13) Prime, K. L.; Whitesides, G. M. Adsorption of Proteins onto Surfaces Containing End-Attached Oligo(ethylene oxide): A Model System Using Self-Assembled Monolayers. *J. Am. Chem. Soc.* **1993**, *115*, 10714–10721.
- (14) Clare, T. L.; Clare, B. H.; Nichols, B. M.; Abbott, N. L.; Hamers, R. J. Functional Monolayers for Improved Resistance to Protein Adsorption: Oligo(ethylene glycol)-Modified Silicon and Diamond Surfaces. *Langmuir* **2005**, *21*, 6344–6355.
- (15) Sofia, S. J.; Premnath, V.; Merrill, E. W. Poly(ethylene oxide) Grafted to Silicon Surfaces: Grafting Density and Protein Adsorption. *Macromolecules* **1998**, *31*, 5059–5070.
- (16) Love, J. C.; Estroff, L. A.; Kriebel, J. K.; Nuzzo, R. G.; Whitesides, G. M. Self-Assembled Monolayers of Thiolates on Metals as a Form of Nanotechnology. *Chem. Rev.* **2005**, *105*, 1103–1169.
- (17) Harder, P.; Grunze, M.; Dahint, R.; Whitesides, G. M.; Laibinis, P. E. Molecular Conformation in Oligo(ethylene glycol)-Terminated Self-Assembled Monolayers on Gold and Silver Surfaces Determines Their Ability to Resist Protein Adsorption. *J. Phys. Chem. B* **1998**, *102*, 426–436.
- (18) Feldman, K.; Haehner, G.; Spencer, N. D.; Harder, P.; Grunze, M. Probing Resistance to Protein Adsorption of Oligo(ethylene glycol)-Terminated Self-Assembled Monolayers by Scanning Force Microscopy. *J. Am. Chem. Soc.* **1999**, *121*, 10134–10141.
- (19) Bain, C. D.; Troughton, E. B.; Tao, Y. T.; Evall, J.; Whitesides, G. M.; Nuzzo, R. G. Formation of Monolayer Films by the Spontaneous Assembly of Organic Thiols from Solution onto Gold. *J. Am. Chem. Soc.* **1989**, *111*, 321–335.
- (20) Li, L.; Chen, S.; Zheng, J.; Ratner, B. D.; Jiang, S. Protein Adsorption on Oligo(ethylene glycol)-Terminated Alkanethiolate Self-Assembled Monolayers: The Molecular Basis for Nonfouling Behavior. *J. Phys. Chem. B* **2005**, *109*, 2934–2941.
- (21) Sun, K.; Song, L.; Xie, Y.; Liu, D.; Wang, D.; Wang, Z.; Ma, W.; Zhu, J.; Jiang, X. Using Self-Polymerized Dopamine to Modify the Antifouling Property of Oligo(ethylene glycol) Self-Assembled Monolayers and Its Application in Cell Patterning. *Langmuir* **2011**, *27*, 5709–5712.
- (22) Krakert, S.; Ballav, N.; Zharnikov, M.; Terfort, A. Adjustment of the Bioresistivity by Electron Irradiation: Self-Assembled Monolayers of Oligo(ethyleneglycol)-Terminated Alkanethiols with Embedded Cleavable Group. *Phys. Chem. Chem. Phys.* **2010**, *12*, 507–515.
- (23) Zorn, S.; Skoda, M. W. A.; Gerlach, A.; Jacobs, R. M. J.; Schreiber, F. On the Stability of Oligo(ethylene glycol) ( $C_{11}EG_6OMe$ ) SAMs on Gold: Behavior at Elevated Temperature in Contact with Water. *Langmuir* **2011**, *27*, 2237–2243.
- (24) Garg, N.; Carrasquillo-Molina, E.; Lee, T. R. Self-Assembled Monolayers Composed of Aromatic Thiols on Gold: Structural Characterization and Thermal Stability in Solution. *Langmuir* **2002**, *18*, 2717–2726.
- (25) Shon, Y.-S.; Lee, T. R. Chelating Self-Assembled Monolayers on Gold Generated from Spiroalkanedithiols. *Langmuir* **1999**, *15*, 1136–1140.
- (26) Shon, Y.-S.; Lee, T. R. A Steady-State Kinetic Model Can Be Used to Describe the Growth of Self-Assembled Monolayers (SAMs) on Gold. *J. Phys. Chem. B* **2000**, *104*, 8182–8191.
- (27) Shon, Y.-S.; Lee, T. R. Desorption and Exchange of Self-Assembled Monolayers (SAMs) on Gold Generated from Chelating Alkanedithiols. *J. Phys. Chem. B* **2000**, *104*, 8192–8200.
- (28) Lee, H. J.; Jamison, A. C.; Lee, T. R. Boc-Protected  $\omega$ -Amino Alkanedithiols Provide Chemically and Thermally Stable Amine-Terminated Monolayers on Gold. *Langmuir* **2015**, *31*, 2136–2146.
- (29) Chinwangso, P.; Jamison, A. C.; Lee, T. R. Multidentate Adsorbates for Self-Assembled Monolayer Films. *Acc. Chem. Res.* **2011**, *44*, 511–519.
- (30) Shon, Y.-S.; Lee, S.; Perry, S. S.; Lee, T. R. The Adsorption of Unsymmetrical Spiroalkanedithiols onto Gold Affords Multi-Component Interfaces That Are Homogeneously Mixed at the Molecular Level. *J. Am. Chem. Soc.* **2000**, *122*, 1278–1281.
- (31) Shon, Y.-S.; Lee, S.; Colorado, R., Jr.; Perry, S. S.; Lee, T. R. Spiroalkanedithiol-Based SAMs Reveal Unique Insight into the Wettabilities and Frictional Properties of Organic Thin Films. *J. Am. Chem. Soc.* **2000**, *122*, 7556–7563.
- (32) Smith, R. K.; Reed, S. M.; Lewis, P. A.; Monnell, J. D.; Clegg, R. S.; Kelly, K. F.; Bumm, L. A.; Hutchison, J. E.; Weiss, P. S. Phase Separation within a Binary Self-Assembled Monolayer on Au{111} Driven by an Amide-Containing Alkanethiol. *J. Phys. Chem. B* **2001**, *105*, 1119–1122.
- (33) Jackson, A. M.; Myerson, J. W.; Stellacci, F. Spontaneous Assembly of Subnanometre-Ordered Domains in the Ligand Shell of Monolayer-Protected Nanoparticles. *Nat. Mater.* **2004**, *3*, 330–336.
- (34) Yaliraki, S. N.; Longo, G.; Gale, E.; Szeleifer, I.; Ratner, M. A. Stability and Phase Separation in Mixed Self-Assembled Monolayers. *J. Chem. Phys.* **2006**, *125*, 074708.
- (35) Fetisov, E. O.; Siepmann, J. I. Structure and Phase Behavior of Mixed Self-Assembled Alkanethiolate Monolayers on Gold Nanoparticles: A Monte Carlo Study. *J. Phys. Chem. B* **2016**, *120*, 1972–1978.

- (36) Tokumitsu, S.; Liebich, A.; Herrwerth, S.; Eck, W.; Himmelhaus, M.; Grunze, M. Grafting of Alkanethiol-Terminated Poly(ethylene glycol) on Gold. *Langmuir* **2002**, *18*, 8862–8870.
- (37) Herrwerth, S.; Eck, W.; Reinhardt, S.; Grunze, M. Factors that Determine the Protein Resistance of Oligoether Self-Assembled Monolayers - Internal Hydrophilicity, Terminal Hydrophilicity, and Lateral Packing Density. *J. Am. Chem. Soc.* **2003**, *125*, 9359–9366.
- (38) Schreiber, F. Structure and Growth of Self-Assembling Monolayers. *Prog. Surf. Sci.* **2000**, *65*, 151–257.
- (39) The incremental increase in film thickness between sulfur and gold, as well as between each of the methylene units, is  $\sim 1.10$  Å, while the thickness variance associated with each OEG unit is  $\sim 2.78$  Å. Therefore, the effective thickness of the overall film ( $(8 \times 1.10) + (3 \times 2.78)$ ) is estimated to be  $\sim 17$  Å.
- (40) Wang, R. L. C.; Kreuzer, H. J.; Grunze, M. Molecular Conformation and Solvation of Oligo(ethylene glycol)-Terminated Self-Assembled Monolayers. *J. Phys. Chem. B* **1997**, *101*, 9767–9773.
- (41) Miller, W. J.; Abbott, N. L. Influence of van der Waals Forces from Metallic Substrates on Fluids Supported on Self-Assembled Monolayers Formed from Alkanethiols. *Langmuir* **1997**, *13*, 7106–7114.
- (42) Colorado, R., Jr.; Lee, T. R. Wettabilities of Self-Assembled Monolayers on Gold Generated from Progressively Fluorinated Alkanethiols. *Langmuir* **2003**, *19*, 3288–3296.
- (43) Allara, D. L.; Nuzzo, R. G. Spontaneously Organized Molecular Assemblies. 1. Formation, Dynamics, and Physical Properties of *n*-Alkanoic Acids Adsorbed from Solution on an Oxidized Aluminum Surface. *Langmuir* **1985**, *1*, 45–52.
- (44) Porter, M. D.; Bright, T. B.; Allara, D. L.; Chidsey, C. E. D. Spontaneously Organized Molecular Assemblies. 4. Structural Characterization of *n*-Alkyl Thiol Monolayers on Gold by Optical Ellipsometry, Infrared Spectroscopy, and Electrochemistry. *J. Am. Chem. Soc.* **1987**, *109*, 3559–3568.
- (45) Snyder, R. G.; Strauss, H. L.; Elliger, C. A. Carbon-Hydrogen Stretching Modes and the Structure of *n*-Alkyl Chains. 1. Long, Disordered Chains. *J. Phys. Chem.* **1982**, *86*, 5145–5150.
- (46) Laibinis, P. E.; Whitesides, G. M.; Allara, D. L.; Tao, Y. T.; Parikh, A. N.; Nuzzo, R. G. Comparison of the structures and wetting properties of self-assembled monolayers of *n*-alkanethiols on the coinage metal surfaces, copper, silver, and gold. *J. Am. Chem. Soc.* **1991**, *113*, 7152–7167.
- (47) Vickerman, J. C. *Surface Analysis: The Principal Techniques*; Wiley: Chichester, U.K., 1997.
- (48) Castner, D. G.; Hinds, K.; Grainger, D. W. X-ray Photoelectron Spectroscopy Sulfur 2p Study of Organic Thiol and Disulfide Binding Interactions with Gold Surfaces. *Langmuir* **1996**, *12*, 5083–5086.
- (49) Hutt, D. A.; Leggett, G. J. Influence of Adsorbate Ordering on Rates of UV Photooxidation of Self-Assembled Monolayers. *J. Phys. Chem.* **1996**, *100*, 6657–6662.
- (50) Biebuyck, H. A.; Bain, C. D.; Whitesides, G. M. Comparison of Organic Monolayers on Polycrystalline Gold Spontaneously Assembled from Solutions Containing Dialkyl Disulfides or Alkanethiols. *Langmuir* **1994**, *10*, 1825–1831.
- (51) Frey, S.; Heister, K.; Zharnikov, M.; Grunze, M.; Tamada, K.; Colorado, R., Jr.; Graupe, M.; Shmakova, O. E.; Lee, T. R. Structure of Self-Assembled Monolayers of Semifluorinated Alkanethiols on Gold and Silver Substrates. *Isr. J. Chem.* **2000**, *40*, 81–97.
- (52) Ishida, T.; Hara, M.; Kojima, I.; Tsuneda, S.; Nishida, N.; Sasabe, H.; Knoll, W. High Resolution X-ray Photoelectron Spectroscopy Measurements of Octadecanethiol Self-Assembled Monolayers on Gold(111). *Langmuir* **1998**, *14*, 2092–2096.
- (53) Tamada, K.; Ishida, T.; Knoll, W.; Fukushima, H.; Colorado, R., Jr.; Graupe, M.; Shmakova, O. E.; Lee, T. R. Molecular Packing of Semifluorinated Alkanethiol Self-Assembled Monolayers on Gold: Influence of Alkyl Spacer Length. *Langmuir* **2001**, *17*, 1913–1921.
- (54) Park, J.-S.; Smith, A. C.; Lee, T. R. Loosely Packed Self-Assembled Monolayers on Gold Generated from 2-Alkyl-2-methylpropane-1,3-dithiols. *Langmuir* **2004**, *20*, 5829–5836.
- (55) Montague, M.; Ducker, R. E.; Chong, K. S. L.; Manning, R. J.; Rutten, F. J. M.; Davies, M. C.; Leggett, G. J. Fabrication of Biomolecular Nanostructures by Scanning Near-Field Photolithography of Oligo(ethylene glycol)-Terminated Self-Assembled Monolayers. *Langmuir* **2007**, *23*, 7328–7337.
- (56) Bain, C. D.; Evall, J.; Whitesides, G. M. Formation of Monolayers by the Coadsorption of Thiols on Gold: Variation in the Head Group, Tail Group, and Solvent. *J. Am. Chem. Soc.* **1989**, *111*, 7155–7164.
- (57) Jeon, S. I.; Lee, J. H.; Andrade, J. D.; De Gennes, P. G. Protein-Surface Interactions in the Presence of Polyethylene Oxide. I. Simplified Theory. *J. Colloid Interface Sci.* **1991**, *142*, 149–158.
- (58) McPherson, T.; Kidane, A.; Szeifer, I.; Park, K. Prevention of Protein Adsorption by Tethered Poly(ethylene oxide) Layers: Experiments and Single-Chain Mean-Field Analysis. *Langmuir* **1998**, *14*, 176–186.
- (59) Zheng, J.; Li, L.; Chen, S.; Jiang, S. Molecular Simulation Study of Water Interactions with Oligo (Ethylene Glycol)-Terminated Alkanethiol Self-Assembled Monolayers. *Langmuir* **2004**, *20*, 8931–8938.
- (60) Ostuni, E.; Chapman, R. G.; Holmlin, R. E.; Takayama, S.; Whitesides, G. M. A Survey of Structure-Property Relationships of Surfaces that Resist the Adsorption of Protein. *Langmuir* **2001**, *17*, 5605–5620.